PHYSICAL REVIEW E **86**, 011711 (2012)

# Surface topography and rotational symmetry breaking

Rajratan Basu,[1,2] Ian R. Nemitz,[1] Qingxiang Song,[3] Robert P. Lemieux,[3] and Charles Rosenblatt[1]
[1]*Department of Physics, Case Western Reserve University, Cleveland, Ohio 44106, USA*
[2]*Department of Physics, U.S. Naval Academy, Annapolis, Maryland 21402, USA*
[3]*Department of Chemistry, Queen's University, Kingston, Ontario, Canada K7L 3N6*
(Received 1 March 2012; published 27 July 2012)

The surface electroclinic effect, which is a rotation of the molecular director in the substrate plane proportional to an electric field $\vec{E}$ applied normal to the substrate, requires both a chiral environment and $C_2$ (or lower) rotational symmetry about $\vec{E}$. The two symmetries typically are created in tandem by manipulating the surface topography, a process that conflates their effects. Here we use a pair of rubbed polymer-coated substrates in a twist geometry to obtain our main result, viz., that the strengths of two symmetries, in this case the rub-induced breaking of $C_\infty$ rotational symmetry and chiral symmetry, can be separated and quantified. Experimentally we observe that the strength of the reduced rotational symmetry arising from the rub-induced scratches, which is proportional to the electroclinic response, scales linearly with the induced topographical rms roughness and increases with increasing rubbing strength of the polymer. Our results also suggest that the azimuthal anchoring strength coefficient is relatively insensitive to the strength of the rubbing.

DOI: 10.1103/PhysRevE.86.011711 PACS number(s): 61.30.Hn

## I. INTRODUCTION

Symmetry plays a central role in many physical phenomena. When two or more symmetries are altered simultaneously, it becomes difficult to quantify the "strengths" of each symmetry individually. Such a case may occur, for example, when a chiral pattern is scribed into a spatially isotropic substrate [1]. The scribing process not only breaks mirror symmetry at the surface, but also breaks the $C_\infty$ rotational symmetry about an axis perpendicular to the surface. When the chiral surface is covered with an achiral nematic liquid crystal, an electroclinic effect (ECE) that is highly localized at the surface obtains [2,3], whereby the nematic director rotates by an angle $\Delta\theta$ in a plane perpendicular, and proportional, to an applied electric field $\vec{E}$. The localized surface rotation $\Delta\theta$ propagates into the bulk liquid crystal, and can be measured by optical techniques with exquisite sensitivity well below $10^{-6}$ rad. But until now it has been very difficult to separate out the consequences of the rubbing-induced rotationally broken symmetry from the rubbing-induced chiral symmetry (the latter typically extending only a few nanometers from the surface [4]), both of which are required for the observation of this phenomenon. In this work we report on an experimental technique that creates the chiral environment using a different approach—a nematic twist cell [5]—which allows us to separate the effects of rotational symmetry breaking from chiral symmetry breaking. In particular, we have quantified the strength of the $C_\infty$ symmetry breaking, which is proportional to the magnitude of the surface electroclinic effect, and find that it scales linearly with the rms surface roughness when the surface is mechanically rubbed, thereby creating parallel scratches that break the $C_\infty$ symmetry. The results demonstrate how one may sort out the individual effects of multiple symmetries acting on a system simultaneously.

Recently we established that a macroscopic mechanical torsional strain can induce molecular-level chirality—actually conformational deracemization—in a configurationally achiral nematic phase [5], thus giving rise to an electroclinic effect. In that work we fabricated a liquid crystal (LC) cell in which the rub-induced easy axes were arranged to induce a near 20° twist of the nematic director from one substrate to the other. The resulting director twist couples to the conformational deracemization of the LC molecules—the left- and right-handed conformers are separated by an energy barrier of $\sim 0.8 k_B T$ [6]—breaking the symmetry between conformations and providing a chiral environment throughout, albeit strongest at the surfaces. Our model [5] suggested that the enantiomer excesses $\varepsilon$ in the bulk and $\varepsilon_s$ at the two surfaces are proportional to the imposed inverse helical pitch $P^{-1}$. Using a special optical geometry to account for the director's helical twist, we measured the surface electroclinic effect in the nematic phase. The susceptibility $d\Delta\theta/dE$, which also is known as the electroclinic coefficient $e_c$, was found to be proportional to the imposed torsional strain, and therefore to the induced chiral strength at the surfaces. But unlike previous methods, this technique [5] allows us to control separately the chiral strength (by changing the imposed twist angle $\theta_0$) and the strength of the $C_\infty$ symmetry breaking (by changing the strength of the polymer rubbing). We therefore adapt this method [5] to control and measure the strength of the rotational symmetry breaking by examining the electroclinic coefficient $e_c$ as a function of rubbing strength for a fixed imposed helical pitch, and thus for a fixed chiral strength.

## II. EXPERIMENTAL

A twist cell was prepared using indium-tin-oxide (ITO) coated glass substrates that were spin coated with the planar-alignment agent RN-1175 polyamic acid (Nissan Chemical Industries). The coated substrates were baked for 60 min at 250 °C. The polyimide surfaces then were rubbed with a cotton pile cloth (YA-20-R, Yoshikawa Chemical Co., Ltd.) attached to the cylindrical roller of an Optron rubbing machine, with roller radius $r = 4$ cm. The average length of the cotton fiber was 1.85 mm, the fiber diameter 6.8 $\mu$m, and fiber density $\sigma_f = 1411$ threads cm$^{-2}$. The substrate was translated at a

 

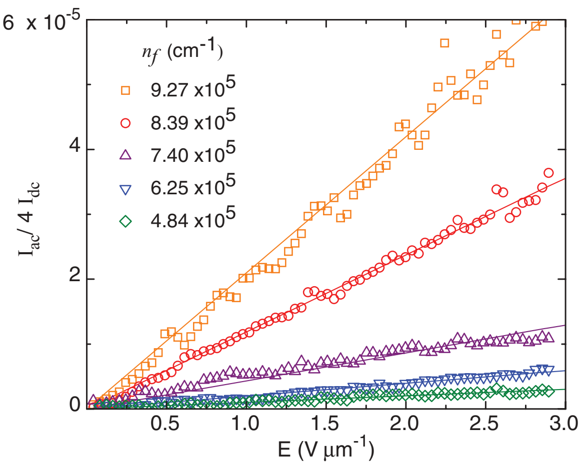


FIG. 1. (Color online) The intensity ratio $I_{ac}/4I_{dc}$ vs applied electric field for five different values of the rubbing strength $n_f$ listed in the legend. The lines represent linear fittings.

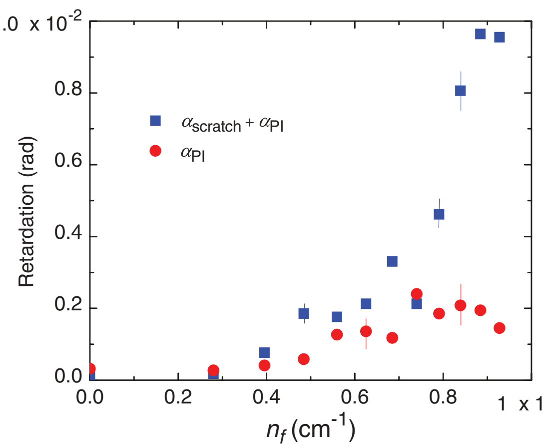


FIG. 2. (Color online) Retardation in air $\alpha_{\rm scratch} + \alpha_{\rm PI}$ and in liquid $\alpha_{\rm PI}$ (red solid circles) vs rubbing strength $n_f$, after subtracting the background retardation at $n_f = 0$.

speed $s = 0.29$ cms$^{-1}$ one time ($N = 1$) beneath the rubbing cylinder, which was rotated at $n = 12$ revolutions s$^{-1}$. In order to achieve a continuous variation of the rubbing strength, the slides were tilted under the rubbing cylinder, such that one end of the slides (at $x = 2.8$ cm) was elevated by an angle of 1.2$^\circ$ on the bed of the rubbing machine. The bed then was raised until the tips of the cotton fibers osculated the slides (with no deformation $\delta$ of the fiber pile, i.e., $\delta = 0$) at position $x = 0.25$ cm (near the lower end of the slide); thus from $x = 0$ to 0.25 cm the rubbing strength $n_f = 0$. Here $n_f$ is defined as the number of fibers passing a position of unit width, and is given by $n_f \approx (2r\delta)^{1/2} 2\pi Nnr\sigma_f/s$ (Ref. [7]). The fiber pile at the elevated end of the slide was deformed by $\delta = 0.058$ cm, such that $\delta$ varied approximately linearly with position along the substrate. Thus, using this gradient rubbing technique, $n_f$ was made to vary monotonically with $x$.

Two gradiently rubbed substrates were placed together to form a cell of thickness $d = 5.2$ $\mu$m, such that their rubbing directions, i.e., their "easy axes," were rotated in the cell's plane by an angle $\theta_0 = (30 \pm 1)^{\rm o}$ with a right-handed twist. The cell was filled with a negative dielectric anisotropy phenyl benzoate liquid crystal 9OO4, the same as used in Ref. [6], which has a phase sequence on cooling, Iso–86°–N–70°–Sm-*A*–62°–Sm-*C*–0°–Sm-*B*–35°–Cryst and a structure given in Ref. [15].

The optical setup for the ECE experiments, which is based on a modification of the classical electroclinic geometry [8] that accounts for the imposed director twist in the cell, is described in detail elsewhere [5]. An ac electric field was applied across the cell, and the detector output was fed into both a dc voltmeter and a lock-in amplifier that was referenced to the driving frequency $f$. The ac intensity $I_{ac}$, its phase relative to $E$, and the dc intensity $I_{dc}$ were computer recorded as $|E|$ was ramped upward with time over 500 s. Figure 1 shows $I_{ac}/4I_{dc}$—this is proportional to the field-induced director rotation $\Delta\theta$ immediately at the substrates [5]—at $f = 1000$ Hz for different values of $n_f$ . The electroclinic coefficients $e_c$ (at $f = 1000$ Hz) vs $n_f$ correspond to the slopes of the data in Fig. 1.

The topography of the gradiently rubbed slides was characterized in two ways: (i) by measuring the optical retardation (the "form retardation") of the rub-induced scratches and (ii) by measuring the surface topography using atomic force microscopy (AFM). Dealing first with method (i), we separated the form retardation $\alpha_{\rm scratch}$ associated with the scratches from the molecular component $\alpha_{\rm PI}$ associated with the alignment of polyimide. To accomplish this, optical retardation measurements of the substrate in air (which facilitate a measurement of $\alpha_{\rm scratch} + \alpha_{\rm PI}$) and the substrate immersed in the near index matching fluid methyl benzoate (Fisher Scientific; which measures $\alpha_{\rm PI}$ only) were performed using a modulated Pockels cell; details are described elsewhere [9,10], and any inherent birefringence in the glass is subtracted out. Figure 2 shows $\alpha_{\rm scratch} + \alpha_{\rm PI}$, as well as $\alpha_{\rm PI}$, as a function of rubbing strength. Note that the difference between the two quantities at a given $n_f$ corresponds to the form retardation $\alpha_{\rm scratch}$. Figure 3(a) shows the dependence of $e_c$ and $\alpha_{\rm scratch}$ on $n_f$. We note that a minimum rubbing strength is required before the onset of scratches; this effectively is a yield stress [11–13].

Images of the rubbed surfaces were made with an Agilent 5500 atomic force microscope. A Veeco model RTESPPW AFM stylus was used in contact mode, where we first made several images to verify that the stylus made no observable change to the surface topography. To obtain quantitative roughness data for the scratches at different $n_f$, we performed scans with a resolution of 1024 pixels and a scanning speed of 0.5 lines s$^{-1}$ over an area of 90 × 90 $\mu$m. The rms roughness, as well as $e_c$, is plotted vs $n_f$ in Fig. 3(b).

## III. DISCUSSION

The frequency-dependent surface electroclinic coefficient $e_c$ for the twist-induced deracemization cell is given by [5]

$$d\Delta\theta/dE = e_c(\omega) = Ce^{-i\omega t}\Big/\Big[W_2^{\varphi} + \sqrt{i\omega\eta K_{22}} \times \tanh\big(d\sqrt{i\omega\eta/K_{22}}/2\big)\Big], \qquad (1)$$

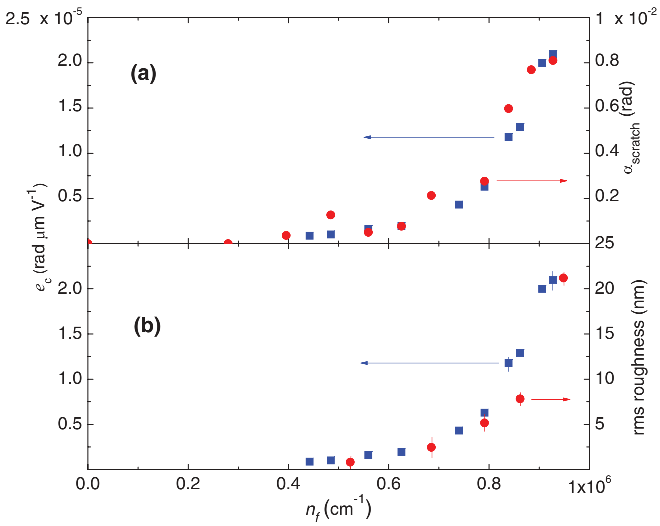


FIG. 3. (Color online) (a) Left axis: The electroclinic coefficient $e_c$ (blue solid squares) vs rubbing strength $n_f$. Right axis: The scratch retardation $\alpha_{scratch}$ (red solid circles) vs $n_f$. (b) Left axis: $e_c$ (blue solid squares) vs $n_f$. Right axis: The rms roughness (red solid circles) vs $n_f$. Error bars for $e_c$ and the rms roughness are shown.

where $C \propto C_{int}\varepsilon_s$, $C_{int}$ is a coefficient that reflects both the chiral interactions between the liquid crystal and alignment layer and the strength of the $C_\infty$ symmetry breaking (i.e., the scratches), $K_{22}$ is the twist elastic constant, $\eta$ is the twist viscosity, and $\omega = 2\pi f$. At $f = 1000$ Hz the second term in the denominator of Eq. (1) dominates and $e_c \propto C \propto C_{int}\varepsilon_s$ for a given cell thickness and frequency. But as noted in Ref. [5], $\varepsilon_s$ is proportional to the deviation $\theta$ of the equilibrium director orientation from the easy axis due to a noninfinite anchoring strength coefficient $W_2^\varphi$, where $W_2^\varphi$ is the coefficient of the surface free energy term quadratic in the deviation of the director's azimuthal orientation from the easy axis direction [14]. Since $\theta = -K_{22}\theta_0/2\left(K_{22} + W_2^\varphi d/2\right)$ (Ref. [5]), we find that the electroclinic coefficient $e_c \propto C_{int}/(K_{22} + W_2^\varphi d/2)$. Taking $K_{22} = 2.5 \times 10^{-12}$ N (Ref. [15]) and a typical value of $W_2^\varphi = 5 \times 10^{-6}$ Jm$^{-2}$ (Ref. [16]), we see that the anchoring term dominates the denominator in the expression for $e_c$, i.e., $e_c \propto C_{int}/W_2^\varphi$.

Our experimental results demonstrate that the electroclinic coefficient increases with rubbing strength $n_f$, as shown in Fig. 1. Figures 3(a) and 3(b) show that $e_c$, which is approximately proportional to $C_{int}/W_2^\varphi$, is proportional to the component of optical retardation $\alpha_{scratch}$ due to the rub-induced striated surface, as well as to the rms topography itself. Turning to the factors $W_2^\varphi$ and $C_{int}$ separately, there is ample evidence from the literature that $W_2^\varphi$ is not strongly sensitive to rubbing strength. Oka *et al.* [17] observed a sharp increase in $W_2^\varphi$ for very weak rubbing (corresponding to $n_f$ approximately one-tenth of the smallest nonzero value used in our experiment), above which $W_2^\varphi$ is almost constant with increasing rubbing strength. Likewise, using an atomic force microscope to scribe a polymer alignment layer, Rastegar *et al.* showed that $W_2^\varphi$ is nearly independent of the vertical scribing force for fixed line separation [18]. The low $n_f$ saturation of $W_2^\varphi$ (Ref. [17]) suggests that the polymer's orientational order parameter at the surface saturates for weak rubbing. But Fig. 2 shows that the optical retardation $\alpha_{PI}$ due to only the alignment of the polymer backbone (but not the surface corrugations) rises slowly with increasing rubbing strength, apparently saturating at large $n_f$. The continued increase of $\alpha_{PI}$ with $n_f$ in Fig. 2 suggests that the interior of the polyimide layer is being heated toward the glass transition temperature [19], and therefore becomes ordered more deeply into the layer with increasing rubbing strength. This results in an increasing integrated birefringence $\alpha_{PI}$ with increasing $n_f$, although not an increase of $W_2^\varphi$.

Thus, assuming that $W_2^\varphi$ in our experiment is approximately constant, we can conclude that $e_c$ is proportional to $C_{int}$. We note that the approximate twofold rotation axis $C_2$ about the normal to the interface becomes a $C_\infty$ in the absence of an easy axis at the substrate. (Because of a very small pretilt of the director at the rubbed surface, the symmetry formally is $C_1$, although this pretilt has been found to have negligible effect [3].) In consequence, in the absence of rubbing the symmetry is too high to support an electroclinic effect, and $C_{int}$ and $e_c$ vanish [Fig. 3(b)]. The appearance of an easy axis when the alignment layer is rubbed breaks the $C_\infty$ rotation, allowing for a nonzero electroclinic coefficient. The apparent scaling of $e_c$ with both the form retardation $\alpha_{scratch}$, which is proportional to the depth of the scratches, as well as to the rms roughness—these represent the same physical phenomenon (scratches)—suggests that strength of the $C_\infty$ symmetry breaking is proportional to the scratch depth. In principle such a result could have been obtained by varying the rubbing strength on an inherently chiral alignment layer, although no such report exists in the literature. Another possible approach would involve using an inherently chiral liquid crystal at a variably rubbed achiral alignment layer. But in this case any surface signal would be overwhelmed by the large bulk electroclinic effect. The only extant result that examines the surface ECE vs rubbing strength comes from our group, where we scribed a chiral pattern into a polyimide alignment layer using an atomic force microscope [1]; this chiral pattern simultaneously served as the easy axis for orientation. There we found that the surface ECE increases with increasing scribing force, although the technique could not distinguish between the effects of scribing on the chiral strength and on the strength of the twofold symmetry axis (i.e., the easy axis) contribution. The present method, on the other hand, facilitates this distinction. Here the chiral strength at the surface is reflected principally in the director deviation $\theta$ from the easy axis, which by polarizing microscope observations was found to vary little with rubbing strength due to the near constant $W_2^\varphi$. Moreover, the strong $n_f$ dependence of our surface ECE—$C_{int}$ is approximately proportional to the rms surface roughness induced by rubbing (and, $e_c \propto C_{int}$)—derives primarily from the strength of the rub-induced $C_\infty$ symmetry breaking, which couples to the chirality and enhances director rotations having the "correct" sense of handedness.

## IV. CONCLUSIONS

In summary, we have demonstrated how the effects of two conflated symmetries can be separated. In particular, we examined the surface nematic electroclinic effect as a function of rubbing strength. We found that above a minimum rubbing strength—this is effectively a yield stress—scratches are created. These striations break the $C_\infty$ rotational symmetry at the surface, which in conjunction with the chiral symmetry induced by the imposed director twist creates a sufficiently reduced symmetry to facilitate a surface electroclinic effect. The strength of the ECE was found to be proportional to the roughness of the topography associated with easy axis scratches. A consequence of this proportionality is that the azimuthal anchoring strength coefficient $W_2^\varphi$ is nearly constant with rubbing strength, consistent with reports in the literature.

## ACKNOWLEDGMENTS

We thank Professor R. G. Petschek for useful discussions. The Case group has support from the National Science Foundation's Condensed Matter Physics and Solid State and Materials Chemistry Programs under Grant No. DMR-1065491. The Queen's group is supported by a Discovery Grant from the Natural Sciences and Engineering Research Council of Canada.

[1] S. Ferjani, J. Pendery, and C. Rosenblatt, Appl. Phys. Lett. **97**, 121905 (2010).
[2] R. F. Shao, J. E. Maclennan, N. A. Clark, D. J. Duer, and D. M. Walba, Liq. Cryst. **28**, 117 (2001).
[3] S. Ferjani, Y. Choi, J. Pendery, R. G. Petschek, and C. Rosenblatt, Phys. Rev. Lett. **104**, 257801 (2010).
[4] R. Berardi, H.-G. Kuball, R. Memmer, and C. Zannoni, J. Chem. Soc., Faraday Trans. **94**, 1229 (1998).
[5] R. Basu, J. S. Pendery, R. G. Petschek, R. P. Lemieux, and C. Rosenblatt, Phys. Rev. Lett. **107**, 237804 (2011).
[6] R. Basu, C. Rosenblatt, and R. P. Lemieux, Liq. Cryst. **39**, 199 (2012).
[7] A. J. Pidduck, G. P. Bryan-Brown, S. D. Haslam, and R. Bannister, Liq. Cryst. **21**, 759 (1996).
[8] G. Andersson, I. Dahl, P. Keller, W. Kuczynski, S. T. Lagerwall, K. Skarp, and B. Stebler, Appl. Phys. Lett. **51**, 640 (1987).
[9] C. Rosenblatt, F. F. Torres De Araujo, and R. B. Frankel, Biophys. J. **40**, 83 (1982).
[10] J.-H. Kim and C. Rosenblatt, Appl. Phys. Lett. **72**, 1917 (1998).
[11] J.-H. Kim and C. Rosenblatt, J. Appl. Phys. **84**, 6027 (1998).
[12] H. Kikuchi, J. A. Logan, and D. Y. Yoon, J. Appl. Phys. **79**, 6811 (1996).
[13] M. P. Mahajan and C. Rosenblatt, Appl. Phys. Lett. **75**, 3623 (1999).
[14] A. Rapini and M. Papoular, J. Phys. (Paris) Colloq. **30**, C4 (1969)
[15] P. G. DeGennes and J. Prost, *Physics of Liquid Crystals* (Clarendon, Oxford, 1994).
[16] M. Vilfan and M. Čopic, Phys. Rev. E **68**, 031704 (2003).
[17] S. Oka, T. Mitsumoto, M. Kimura, and T. Akahane, Phys. Rev. E **69**, 061711 (2004).
[18] A. Rastegar, M. Škarabot, B. Blij, and Th. Rasing, J. Appl. Phys. **89**, 960 (2001).
[19] H. Mada and T. Shinoda, Jpn. J. Appl. Phys. **32**, 1245 (1993).